Guided ion-beam studies of the kinetic-energy-dependent reactions of Co_n^+ (n=2–16) with D_2: Cobalt cluster-deuteride bond energies

Fuyi Liu and P. B. Armentrout[a)]
Department of Chemistry, University of Utah, Salt Lake City, Utah 84112

(Received 14 February 2005; accepted 10 March 2005; published online 19 May 2005)

The kinetic-energy-dependent cross sections for the reactions of Co_n^+ (n=2–16) with D_2 are measured as a function of kinetic energy over a range of 0–8 eV in a guided ion-beam tandem mass spectrometer. The observed products are Co_nD^+ for all clusters and $Co_nD_2^+$ for n=4,5,9–16. Reactions for the formation of Co_nD^+ (n=2–16) and $Co_9D_2^+$ are observed to exhibit thresholds, whereas cross sections for the formation of $Co_nD_2^+$ (n=4,5,10–16) exhibit exothermic reaction behavior. The Co_n^+–D bond energies as a function of cluster size are derived from the threshold analysis of the kinetic-energy dependence of the endothermic reactions and are compared to previously determined metal–metal bond energies, $D_0(Co_n^+–Co)$. The bond energies of Co_n^+–D generally increase as the cluster size increases, and roughly parallel those for Co_n^+–Co for clusters $n \geqslant 4$. These trends are explained in terms of electronic and geometric structures for the Co_n^+ clusters. The bond energies of Co_n^+–D for larger clusters ($n \geqslant 10$) are found to be very close to the value for chemisorption of atomic hydrogen on bulk-phase cobalt. The rate constants for D_2 chemisorption on the cationic clusters are compared with the results from previous work on cationic and neutral cobalt clusters. © *2005 American Institute of Physics*. [DOI: 10.1063/1.1899604]

I. INTRODUCTION

The interaction of dihydrogen with metal surfaces has been widely investigated[1,2] because hydrogen absorption and reactions often play a decisive role in fuel cell and energy storage technology, material science, and heterogeneous catalysis. Transition-metal clusters are often characterized by a high degree of coordinative unsaturation with a number of dangling bonds and, therefore, can act as an ideal model of dispersed catalytic surfaces. A better understanding of the catalytic activity at the molecular level is expected to be valuable in designing new and more effective catalysts. Studies of the reactivity of transition-metal clusters can provide insight into the relation between geometric or electronic structure and chemical reactivity, which can exhibit an appreciable dependence on cluster size, charge state, and elemental identity.[3–6] A number of absorption and reaction studies have been reported previously for cobalt clusters[7–22] in part because cobalt is an important catalytic metal in many industrial processes.[23,24] These include Fischer–Tropsch synthesis, in which larger hydrocarbons are produced from carbon monoxide and hydrogen.[25,26]

The reactions of neutral and charged cobalt clusters with hydrogen/deuterium have been investigated extensively by several groups. Smalley and co-workers[7,8] have studied the reactions of neutral cobalt clusters with D_2 using a fast-flow reaction tube. They measured the relative reaction-rate constants for D_2 dissociation on various-sized clusters and found a strong reactivity dependence on cluster size. The atom and dimer do not react with D_2, clusters for n=4–9 exhibit low reactivity with a minimum at n=6, whereas n=3, 10–28 clusters react much more efficiently. Ho *et al.*[9] investigated the gas-phase reaction and saturation absorption on the surface of neutral cobalt clusters, n=7–68, and found a similar reactivity dependence on cluster size for the cluster sizes reported by Smalley and co-workers. The authors also determined the absolute rate constants and reaction probabilities, and examined the temperature dependence of the rate constants for the dissociative adsorption of the first D_2 molecule to cobalt clusters Co_n (n=9–21) over the temperature range of 133–373 K.[9] The rate constants for clusters n=10–13, 15–17 show no dependence on temperature, indicating that D_2 chemisorption reaction has no activation barrier; whereas the rate constants for Co_9 and Co_{14} increase at higher temperatures, which suggests the presence of activation barriers (8.8 and 7.8 kJ/mol, respectively). This group also studied very large clusters, n=55–147, reacting with D_2, finding evidence for icosahedral structures and a ratio of D atoms to surface metal atoms near unity.[10] Persson *et al.*[11] also reported the reactivity of neutral cobalt clusters with n =10–45 with D_2 using two reaction cells under near single-collision conditions. They determined the reaction probability for adsorption of the first and second D_2 molecule using a statistical model. The size dependence of the Co_n–D_2 reaction system was found to correspond well with the observations from the fast-flow reactor experiments of the Smalley and Riley groups.

Nakajima *et al.*[12] investigated the reactivity of positively charged cobalt cluster ions Co_n^+ (n=2–22) with H_2 by using a fast-flow reactor. They compared the reactivities of the corresponding neutral and cationic cobalt clusters with D_2 and

a)Electronic mail: armentrout@chem.utah

found similar efficiencies for larger clusters. This result suggests that removing an electron from the dense orbital manifold of larger neutral clusters ($n \geq 8$), which have a high density of valence electronic states, should have little effect. However, the reactivities of Co_n^+ ($n=4$–9) were found to be much higher than their neutral analogs. Apparently, the positive charge dramatically affects the reactivities of these smaller clusters.

Although these size- and temperature-dependent investigations of reactivity are interesting, previous work is limited to thermal reactions. Consequently, studies of the thermochemistry of dihydrogen reactions with cobalt clusters are scarce. In the present study, we use guided ion-beam tandem mass spectrometry to investigate the reactions of size-selected cobalt cluster cations Co_n^+ ($n=2$–16) with D_2. Kinetic-energy-dependent cross sections for the formation of $Co_nD^+ + D$ and $Co_nD_2^+$ product channels are determined. The former are interpreted to provide Co_n^+–D bond dissociation energies (BDEs) as a function of cluster size. Bond energy information for the larger clusters obtained here is favorably compared to bulk-phase values. The rates of D_2 chemisorption on the cationic clusters are compared with the results from previous work.[7–12] This study is a continuation of our efforts to provide quantitative measurements of the thermodynamics and reactivities of transition-metal clusters, which have shown interesting variations with cluster size in the stability and reactivity of clusters. Hence the results obtained here are briefly compared to comparable studies of the reactions of D_2 with cluster cations of Fe, Cr, V, and Ni.[27–30]

II. EXPERIMENTAL SECTION

The experimental apparatus and techniques in this study have been described in detail elsewhere,[31] and only a brief description is given here. Cluster cations are formed by laser vaporization of a cobalt rod housed in an aluminum source block.[32,33] The output (511 and 578 nm) of an Oxford ACL 35 copper vapor laser operating at 7 kHz is tightly focused onto a continuously translating and rotating cobalt rod to expose fresh surface to the laser. The optimum pulse energy for cobalt cluster-ion production ranges between 3 and 4 mJ/pulse. The vaporized material is entrained in a continuous flow [$(5–6)\times 10^3$ SCCM (standard cubic centimeter per minute)] of He passing over the ablation surface. Frequent collisions and rapid mixing lead to the formation of thermalized clusters as they travel down a 2-mm-diameter $\times$63-mm-long condensation tube. This seeded helium flow then undergoes a mild supersonic expansion and passes through a skimmer in field-free conditions. Previous studies have indicated that the clusters are not internally excited and likely to be near room temperature,[31,34] although direct measurements of the internal temperatures of the clusters are not possible.

Positively charged ions pass through two differentially pumped regions and are accelerated and focused into a 60° magnetic sector momentum analyzer. The mass-selected ions are decelerated and injected into a rf octopole ion guide[35,36] that extends through a reaction cell. The octopole beam guide is biased with dc and rf voltages. The former allows accurate control of the translational energy of the incoming ions, whereas the latter establishes a radial potential that efficiently traps the parent and product ions that travel through the octopole. The pressure of D_2 neutral reactant gas (Cambridge Isotope Labs., 99.8% purity) in the reaction cell is kept relatively low to reduce the probability of multiple collisions with the ions. To test this, all the studies were conducted at two pressures of D_2, ~0.2 and ~0.4 mTorr. The product and reactant ions drift to the end of the octopole, where they are extracted, and injected into a quadrupole mass filter for mass analysis. Ion intensities are measured with a Daly detector[37] coupled with standard pulse counting techniques. Reactant ion intensities ranged from 1 to 5 $\times 10^6$ ions/s. The observed product intensities are converted to absolute reaction cross sections as discussed in detail elsewhere.[36] The absolute errors in the cross sections are on the order of ±30%. The products observed in this work include Co_nD^+ and $Co_nD_2^+$ species. Accurate measurements of the intensities of these species are most conveniently accomplished by using deuterium to maximize the peak separation and by adjusting the resolution of the quadrupole mass filter to be as high as possible without reducing the product ion intensities. In all cases, the cross sections reported below have been corrected for mass overlap with other species.

The results for each reaction system were repeated several times to ensure their reproducibility. Collision-induced dissociation (CID) experiments with Xe were performed on all cluster ions to ensure their identity and the absence of any excessive internal excitation. In all instances, CID thresholds are consistent with those previously reported.[34] The absolute zero in the kinetic energy of the ions and their energy distributions (0.7–1.8 eV, gradually increasing with cluster size) were measured using the octopole as a retarding energy analyzer.[36] The error associated with the zero of the absolute energy scale is 0.05 eV in the laboratory frame. Kinetic energies in the laboratory frame are converted to center-of-mass (CM) energies using the stationary target approximation, $E(\mathrm{CM})=E(\mathrm{lab})m/(m+M)$, where m and M are the masses of the neutral and ionic reactants, respectively. The data at the lowest energies are corrected for truncation of the ion-beam energy distribution.[36]

III. RESULTS

Figure 1 shows the kinetic-energy dependence of the cross sections for reaction of Co_n^+ ($n=2$–16) with D_2 over a range of thermal to as high as 8 eV (eventually limited by 1 kV laboratory). Despite a careful search for products with fewer cobalt atoms, the only products observed were those formed in reactions (1) and (2).

$$Co_n^+ + D_2 \rightarrow Co_nD^+ + D, \tag{1}$$

$$\rightarrow Co_nD_2^+. \tag{2}$$

Only reaction (1) is observed for clusters with $n=2$, 3, 6–8, whereas both reactions are observed for clusters with $n=4$, 5, 9–16. Reaction (1) exhibits a threshold in all cases, whereas reaction (2) is barrierless except for $n=9$. The resultant cross sections exhibited no pressure dependence for all cluster

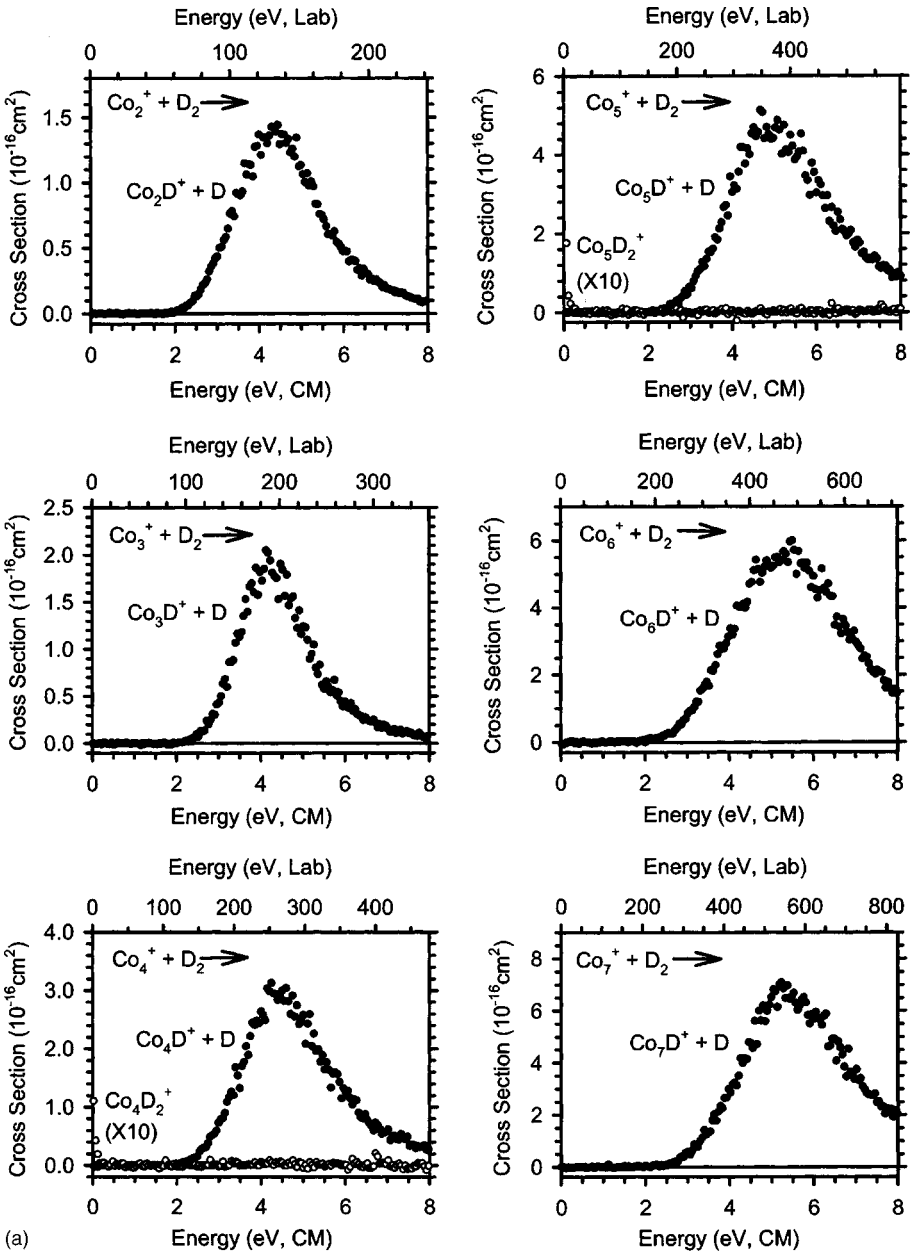

FIG. 1. Cross sections for reactions of Co_n^+ (n=2–16) with D_2 as a function of collision energy in the center-of-mass (lower x axis) and laboratory (upper x axis) frames.

sizes, verifying that the results presented here result exclusively from single ion-molecule collisions.

Similar to the results for reactions of D_2 with iron,[27] chromium,[28] vanadium,[29] and nickel[30] cluster ions, we fail to observe collision-induced dissociation of the cobalt cluster ions with D_2. These observations can be explained by previous work in our laboratory that has shown that CID processes are inefficient for target gases (such as D_2) with low masses and polarizabilities.[38,39] Also, we observed no products with fewer cobalt atoms than the reactants, such as $Co_{n-1}D_2^+$ or $Co_{n-1}D^+$. This indicates that the $Co_nD_2^+$ and Co_nD^+ products decompose preferentially by loss of D_2 or D, respectively, rather than Co atom loss.

A. Cross sections for Co_nD^+ formation

The formation of Co_nD^+ in reaction (1) is observed to be endothermic for all clusters studied (Fig. 1). The kinetic-energy dependences of the cross sections are similar to those previously reported for Fe_n^+, Cr_n^+, V_n^+, and Ni_n^+ clusters reacting with D_2.[27–30] The cross sections exhibit apparent thresholds of 2.0±0.5 eV for all clusters and reach maxima at 4–6 eV. The decline in the formation of Co_nD^+ at elevated energies can be attributed to the overall reaction (3),

$$Co_n^+ + D_2 \rightarrow Co_nD^+ + D \rightarrow Co_n^+ + 2D, \quad (3)$$

which can begin at $D_0(D_2)$=4.56 eV.[40] Smaller clusters exhibit an onset for this reaction close to its thermodynamic limit, 4.56 eV minus the internal energy of the cluster reactants. Figure 1 shows that the cross-section maximum moves to higher energies as the cluster size increases, which can be attributed to kinetic shifts in this process. Larger clusters are able to accommodate more excess energy, so that the lifetime of the Co_nD^+ product increases with increasing cluster size and eventually becomes larger than the 10^{-4} s time window

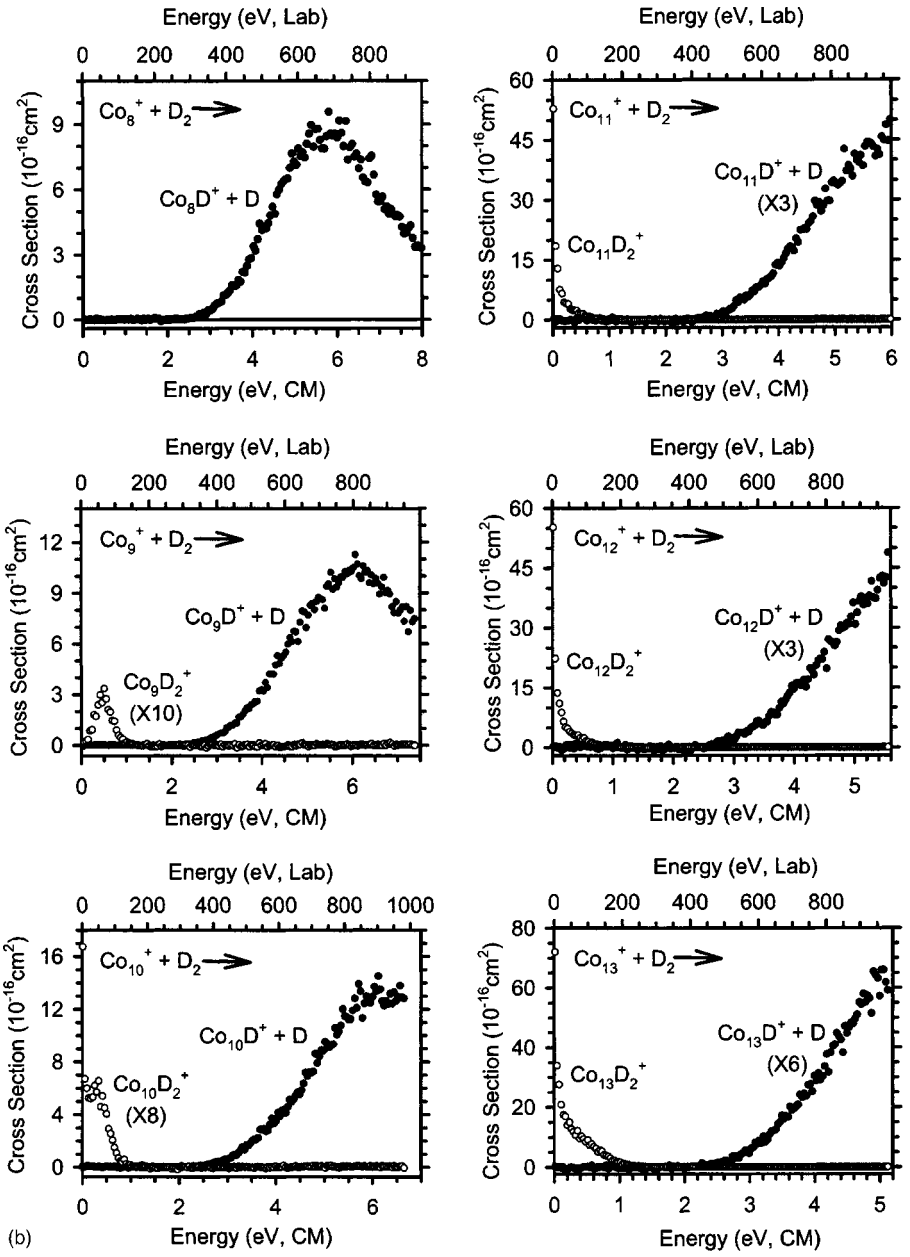

FIG. 1. (*Continued*).

available for dissociation in our experimental apparatus. At higher kinetic energies, the lifetime for dissociation becomes shorter than this time window and the dissociation process is again observed as declines in the Co_nD^+ cross sections. Note that the observation of maxima in the Co_nD^+ cross sections corresponding to reaction (3) is consistent with the failure to observe Co_mD^+ products, where $m<n$, i.e., Co_nD^+ clusters preferentially dissociate by losing D rather than Co atoms. Qualitatively, this result shows that Co_n^+–D bonds are weaker than DCo_{n-1}^+–Co bonds.

The absolute magnitude of the reaction cross section for Co_2^+ is comparable to that previously observed for reaction of ground-state $Co^+(^3F, 3d^8)$.[41] The cross-section magnitudes for Co_n^+ gradually increase with cluster size, being about an order of magnitude larger for the largest clusters studied. The fact that the reaction probability increases with increasing cluster size is consistent with larger collision cross sections for the physically larger clusters. This indicates that the electronic requirements necessary for the reaction of D_2 with Co_n^+ clusters are similar or enhanced compared to those for $Co^+(^3F, 3d^8)$. Thus cluster orbitals of appropriate symmetries and occupancies are available to interact with the σ and σ^* orbitals of D_2.[42,43]

B. Cross sections for $Co_nD_2^+$ formation

The smallest clusters for which dideuteride products are observed are Co_4^+ and Co_5^+, as shown in Figs. 1 and 2, but the cross sections are quite small $[(0.1–0.2)\times 10^{-16}$ cm^2 near zero energy]. Surprisingly dideuteride products are not observed for clusters $n=6–8$. The cross section for $Co_9D_2^+$ increases in magnitude with increasing energy, behavior indicating a barrier to the reaction or possibly an endothermic process. The $n=11–13$ and 15 cluster cations as well as clus-

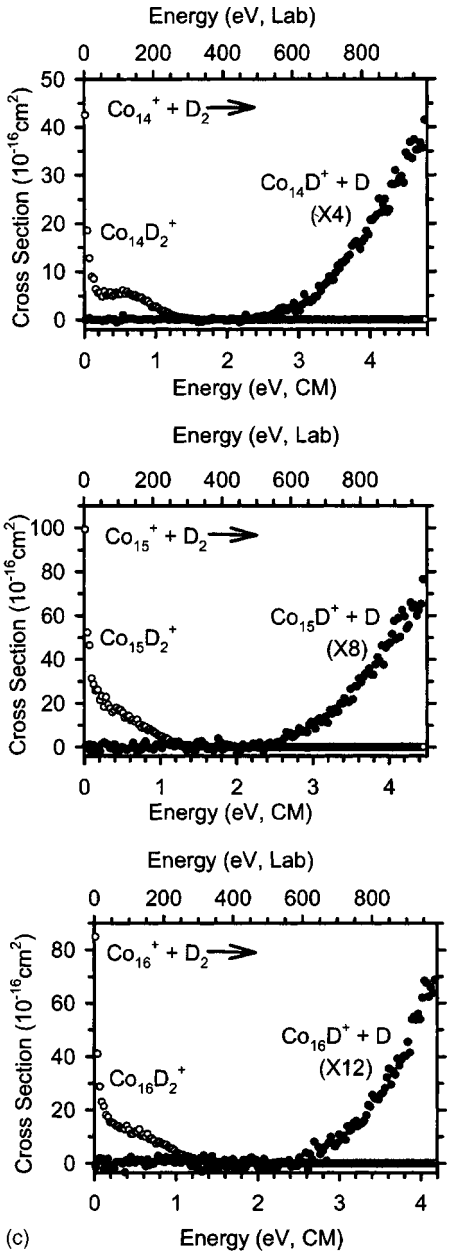

FIG. 1. (*Continued*).

ters $n=4$ and 5 display $Co_nD_2^+$ cross sections that decrease monotonically with increasing energy. This behavior is most easily seen on the logarithmic scale of Fig. 2, where at lower energies these cross sections decline as $E^{-0.9\pm0.1}$ for $n=11$ and 12, as $E^{-0.6\pm0.1}$ for $n=13$ and 15, and as $E^{-0.8\pm0.1}$ for $n=4$, whereas the points available for $n=5$ are too sparse to get an accurate energy dependence. Such monotonic declines in cross section are characteristic behavior of exothermic ion-molecule reactions. In contrast, the $n=10$ and 14 cluster cations are found to have cross sections exhibiting both obvious exothermic and endothermic features (Fig. 2). Although more subtle, the cross section of $Co_{16}D_2^+$ declines roughly as $E^{-0.7}$ at lower energies, but above about 0.1 eV, the magnitude of the cross section declines more slowly, again suggesting that there are both endothermic and exothermic features present. In addition, the magnitudes of the cross sections for $Co_nD_2^+$ ($n=4$, 5, 9–16) generally increase

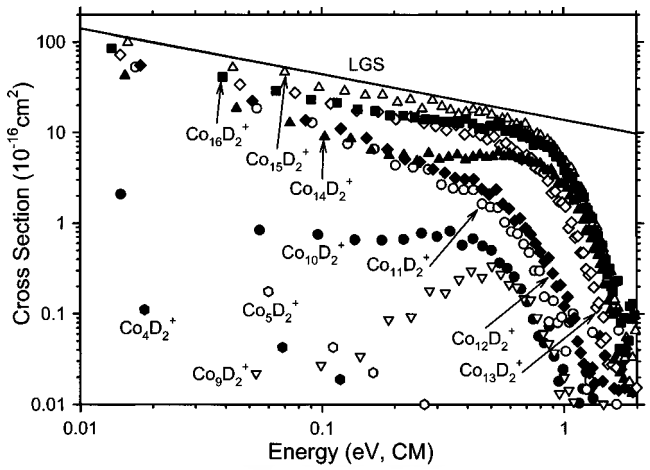

FIG. 2. Cross sections for reaction (2) plotted on a log scale for $n=4$, 5, 9–16 as a function of collision energy in the center-of-mass frame. The solid line indicates the LGS model cross section (Ref. 44).

as the cluster size increases in the low-energy range except that $Co_{14}D_2^+$ and $Co_{16}D_2^+$ have cross sections smaller than neighboring clusters. The cross sections decline roughly as $E^{-1/2}$ at lower energies (Fig. 2) although the data point densities for $Co_4D_2^+$ and $Co_5D_2^+$ are too low to ascertain the energy dependence quantitatively. Such behavior conforms to the $E^{-1/2}$ energy dependence predicted for ion-molecule collisions by the Langevin–Gioumousis–Stevenson (LGS) model.[44] The cross-section magnitudes for $Co_nD_2^+$ ($n=11$–16) are close to the LGS model prediction at the lower energies.

With increasing interaction energy, the magnitudes of all $Co_nD_2^+$ cross sections decline more rapidly (about as $E^{-5.5\pm1.0}$ for $n=10$–16). These declines can be attributed to the overall reaction (4), as no other dissociation process is energetically accessible.

$$Co_n^+ + D_2 \rightarrow Co_nD_2^+ \rightarrow Co_n^+ + D_2. \quad (4)$$

No energy is required for this overall process as the products are the same as the initial reactants. We believe that the more rapid decline in the cross sections is governed by the changing lifetime of the intermediate, which decreases as the interaction energy increases and increases with the cluster size. Observation of the $Co_nD_2^+$ product is expected only if its lifetime exceeds or is on the order of the detection time window of our instrument, $\sim10^{-4}$ s. The reason that we do not observe any $Co_nD_2^+$ products for many smaller clusters ($n=2$, 3, 6–8) is probably because these species dissociate more rapidly than this time window, even at low kinetic energies. As discussed further below, the observation of $Co_4D_2^+$ and $Co_5D_2^+$ near zero energy results from the higher reactivity of the Co_4^+ and Co_5^+ clusters, as also previously observed by Nakajima *et al.*[12]

The $Co_nD_2^+$ product ions can conceivably have one of two forms: (1) a physisorbed state, a weakly bound adduct held together by ion-induced dipole attractions; or (2) a dissociative chemisorbed state, a strongly bound species where both deuterium atoms are chemically bonded to the cluster. We have previously argued[27–30] that a weakly bound adduct in which the D_2 molecule was intact should allow reaction

(4) to be kinetically facile as well as being thermodynamically allowed at all collision energies. Consequently, it is difficult to understand how such a weakly bound physisorbed species can survive our instrumental flight time of 10^{-4} s, unless it is collisionally stabilized by multiple collisions with D_2. Our pressure-dependent studies verify that the $Co_nD_2^+$ products are not the result of collision stabilization. Therefore, the formation of $Co_nD_2^+$ products does not behave as expected for a physisorption process. However, if the $Co_nD_2^+$ clusters are dissociatively chemisorbed species, then reaction (4) requires that the two deuterium atoms come back together and pass through a transition state associated with cleaving the cluster-deuterium bonds and forming a D_2 bond. Such a process should be kinetically hindered, especially for larger clusters where the chemisorption energy can be dissipated throughout the cluster. This would explain the long lifetimes observed for $Co_nD_2^+$ (n=4, 5, 9–16) products and why the magnitudes of the $Co_nD_2^+$ cross sections increase for larger clusters. Clearly, chemisorption of D_2 is efficient for the larger clusters ($n \geqslant 11$).

IV. THRESHOLD ANALYSIS AND THERMOCHEMISTRY

A. Data analysis

The energy dependences of cross sections for endothermic processes in the threshold region are analyzed using the methods detailed previously.[45–47] Briefly, the threshold region is modeled using Eq. (5)

$$\sigma(E) = \sigma_0 \sum g_i(E + E_i - E_0)^N/E, \quad (5)$$

where σ_0 is an energy-independent scaling parameter, N is an adjustable parameter, E is the relative kinetic energy, and E_0 is the threshold for reaction at 0 K. The model includes the average vibrational and rotational energies of clusters ions at 300 K, which are evaluated from the respective cluster frequencies and rotational constants by summing over the rovibrational states having energies E_i and relative populations g_i, where $\Sigma g_i = 1$. The model cross section, Eq. (5), is also convoluted with the kinetic-energy distributions of the ion and neutral reactants before comparison to the experimental data.[36]

For metal clusters, it has been shown that lifetime effects become increasingly important as the size of the cluster increases.[48] This is because metal clusters have many low-frequency vibrational modes such that the lifetime of the transient intermediate can exceed the experimental time available for reaction (approximately 10^{-4} s in our apparatus). Thus, an important component of the modeling of these reactions is to include the effect of the lifetime of the reaction, as estimated using statistical Rice–Ramsperger–Kassel–Marcus (RRKM) theory.[49–51] The method to incorporate lifetime effects in our modeling has been discussed in detail previously.[52] The formation of Co_nD^+ products from the $Co_nD_2^+$ intermediate probably occurs via a loose transition state (LTS) located at the centrifugal barrier, which is treated variationally as described in detail elsewhere.[52] For ion-molecule reactions having no barriers in excess of the reaction endothermicity, this phase-space limit (PSL) is a reasonable assumption.[49] However, covalent bond cleavage may be better represented by a tighter transition state.[28–30,53] Therefore, we also considered a tight transition state (TTS) model where we simply remove the frequency corresponding to the reaction coordinate, a cluster-D stretch. These two models should provide conservative lower and upper limits to the dissociation rates for D atom loss from the $Co_nD_2^+$ intermediates.

When we model the cross sections with RRKM theory, molecular constants for the energized molecule (EM) and transition state (TS) leading to the products, and the reaction degeneracy (two for loss of D from the $Co_nD_2^+$ intermediate) are required. For the primary reaction leading to Co_nD^+, the energized molecule is the transiently formed $Co_nD_2^+$ complex, which we assume has a DCo_nD^+ structure. For all the species, the $3n$-6 vibrations associated with the metal cluster are assumed to equal those of the bare cluster and calculated by using an elastic cluster model suggested by Shvartsburg *et al.*[54] In this study, the parameters used are the Debye frequency for bulk cobalt, $\nu_D(\infty)$=280 cm^{-1}, the bulk maximum longitudinal frequency, $\nu_{L,\,max}$=301 cm^{-1}, and the ratio of the longitudinal to the transverse phonon velocity, c_L/c_T =1.81, which are estimated from the average values of bulk nickel[55,56] and bulk iron,[56–58] respectively. For the DCo_nD^+ intermediates and Co_nD^+ products, six and three additional frequencies, respectively, are needed and are estimated as follows. In $Co_nD_2^+$, we assume both deuterium atoms bind to two chemically equivalent bridging positions, although this assumption is not critical to the final results obtained. To obtain the asymmetric stretch frequency for DCo_n^+–D and Co_n^+–D, we first compare the asymmetric stretching frequencies determined experimentally for DFe–D (1200 cm^{-1}) (Ref. 59) and for DCo–D (1220 cm^{-1}),[60] where the values are the average of frequencies measured in Kr and Ar matrices in both cases. This ratio (1.02) is used to scale frequencies previously estimated for DFe_n^+–D.[27] This gives values of 885 cm^{-1} for the asymmetric stretch, 966 cm^{-1} for the symmetric stretch, and 737 cm^{-1} for the wag. Although these procedures may be over simplified, the magnitudes of the errors associated with these estimates of frequencies were evaluated by scaling all the frequencies by ±50%, which produces differences in the thresholds that are less than 0.04 eV.

Modeling of the Co_nD^+ product cross sections includes energies above the point where the cross section declines as a result of product dissociation, reaction (3). Including this region in our data analysis is advantageous because the more extensive energy range helps constrain the parameters in Eq. (5). This dissociation process can be modeled using simple statistical assumptions that are outlined elsewhere[61] and have been used successfully to describe the high-energy behavior of the $Co^+ + D_2 \rightarrow CoD^+ + D$ reaction.[41] Briefly, Eq. (5) is multiplied by an energy-dependent probability factor for product dissociation that depends on two adjustable parameters: E_D, the dissociation energy and, p, an empirical fitting parameter. For the reactions considered here, E_D is just the D_2 dissociation energy, 4.56 eV. Values of p ranging from 1 to 5 were tested and a value of p=4 was found to best reproduce the data for most of the clusters.

TABLE I. Summary of parameters used in Eq. (5) for the analysis of Co_nD^+ cross sections. (Uncertainties in parentheses.)

n	σ_0[a]	N[a]	E_0(TTS)eV[b]	E_0(PSL)eV[c]	$D_0(Co_n^+–D)$eV[d]
1		1.1(0.1)[e]		2.53(0.06)[e]	2.03(0.06)[e]
2	3.1(0.3)	1.3(0.1)	2.21(0.09)	2.21(0.08)	2.35(0.09)
3	6.1(0.8)	1.5(0.2)	2.57(0.11)	2.58(0.11)	1.99(0.11)
4	4.5(0.8)	1.9(0.2)	2.27(0.12)	2.35(0.12)	2.25(0.16)
5	6.0(1.4)	1.9(0.2)	2.32(0.11)	2.50(0.15)	2.15(0.23)
6	6.0(1.6)	1.7(0.1)	2.17(0.16)	2.41(0.17)	2.27(0.29)
7	7.2(1.8)	1.9(0.2)	2.24(0.14)	2.55(0.12)	2.17(0.29)
8	9.1(2.0)	1.9(0.2)	2.20(0.11)	2.54(0.14)	2.19(0.31)
9	7.7(1.9)	2.0(0.2)	2.00(0.11)	2.41(0.12)	2.36(0.33)
10	7.8(1.5)	2.0(0.1)	1.86(0.10)	2.33(0.11)	2.47(0.35)
11	11.6(2.7)	1.8(0.2)	1.87(0.11)	2.31(0.14)	2.47(0.36)
12	12.0(2.5)	1.8(0.1)	1.80(0.10)	2.27(0.13)	2.53(0.37)
13	10.7(2.1)	1.9(0.2)	1.67(0.09)	2.14(0.11)	2.65(0.35)
14	11.3(2.3)	1.9(0.1)	1.66(0.08)	2.15(0.10)	2.67(0.35)
15	16.6(2.4)	1.8(0.2)	1.63(0.07)	2.14(0.10)	2.67(0.35)
16	14.7(2.0)	1.8(0.2)	1.61(0.07)	2.14(0.10)	2.69(0.37)

[a]Values for PSL (LTS) model. TTS parameters are similar.
[b]Tight transition state (TTS) model described in text.
[c]PSL (LTS) model described in text.
[d]Average value derived from TTS and PSL (LTS) thresholds according to Eq. (6).
[e]Value from Ref. 41.

B. Thresholds and thermochemical results

The optimum values of the parameters of Eq. (5), E_0, σ_0, and N, used to reproduce the cross sections for the monodeuteride products are given in Table I. Co_nD^+ product cross sections are modeled using both loose (PSL) and tight transition states, as described above. A representative fit of the data for the monodeuteride product ions is shown in Fig. 3. Given the assumption that there are no barriers in excess of the endothermicities to the formation of Co_nD^++D, the thresholds for reaction (1), $E_0(1)$, can be converted to Co_n^+–D bond energies according to Eq. (6),

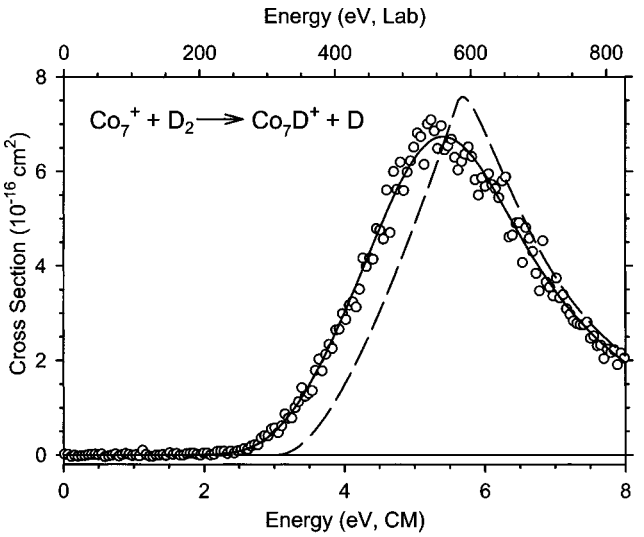

FIG. 3. Cross section for reaction (1) with $n=7$ as a function of collision energy in the center-of-mass (lower x axis) and laboratory (upper x axis) frames. The dashed line shows the model of Eq. (5) with optimized parameters from Table I and also includes RRKM lifetime effects and the model for product dissociation. The solid line shows the model after convolution over the neutral and ion kinetic and internal energy distributions.

$$D_0(Co_n^+–D) = D_0(D_2) - E_0(1). \quad (6)$$

Because the model of Eq. (5) explicitly accounts for the internal and translational energy distributions of the reactants, the thermochemistry derived corresponds to 0 K. The bond energies calculated in this manner are given in Table I, as an average of values derived from thresholds obtained using kinetic shifts modeled with loose (PSL) and tight TS assumptions.

The assumption that there are no barriers to reaction (1) in excess of the endothermicity has proved to be valid for many ion-molecule reactions because the long-range ion-induced dipole interactions between ions and polarizable neutrals are attractive. Exceptions often involve restrictions in spin or orbital angular momentum.[46,62] Unfortunately, conservation of such quantities cannot be examined for the present systems because detailed information concerning the electronic states of both reactants and products is not available. However, transition-metal clusters have a dense manifold of electronic states, such that we believe interactions (such as spin-orbit mixing) among these surfaces should allow adiabatic pathways for product formation without barriers in excess of the endothermicities for Co_nD^+. Thus, we assume that the thresholds for reactions leading to the formation of Co_nD^+ represent the adiabatic endothermicities. Indirect evidence for the validity of this assumption is the correspondence between the cluster and bulk-phase bond energies to hydrogen, as elucidated below.

V. DISCUSSION

A. Co_n^+–D bond energies

Table I lists the thresholds derived from the analysis of the Co_nD^+ cross sections using Eq. (5), assuming both loose and tight transition states. Both sets of energies show the

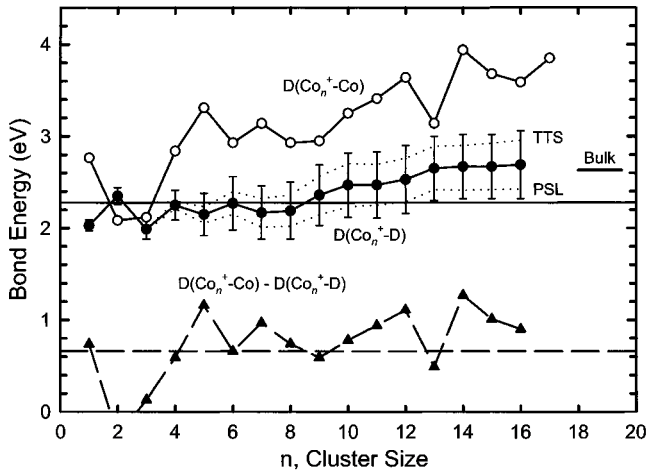

FIG. 4. $D_0(Co_n^+–D)$ (●, Table I), $D_0(Co_n^+–Co)$ (◯, Ref. 34), and the difference, $D_0(Co_n^+–Co)–D_0(Co_n^+–D)$ (▲), plotted as a function of cluster size n. The horizontal solid line at 2.28 eV indicates half of the $D_0(D–D)$ bond energy. The two dotted lines indicate the upper and lower limits to the $Co_n^+–D$ bond energies obtained by analysis using TTS and PSL models. The horizontal line labeled bulk indicates the average of the experimental binding energies of H to Co(0001) and Co(1010) surfaces (Refs. 2,67,68).

same oscillations with cluster size. Relative to the TTS values, thresholds obtained using the PSL model are the same for Co_2^+ and Co_3^+, and then gradually increase. They are an average of 0.23±0.10 eV higher than the TTS values for n =4–8, and 0.48±0.05 eV for $n \geqslant 9$. The loose and tight transition state models provide conservative upper and lower limits to the threshold energies, respectively.

The bond energies of $Co_n^+–D$ are derived from the thresholds measured here using Eq. (6). Conservatively, we take our best values for the $Co_n^+–D$ bond energies as the average of those derived using Eq. (5) from the TTS and PSL threshold energies. This parallels our treatment for $Cr_n^+–D$, $V_n^+–D$, and $Ni_n^+–D$ bond energies.[28–30] These average values of $Co_n^+–D$ bond energies are listed in Table I and shown in Fig. 4 along with uncertainties increased to reflect the span of values. Note that the listed uncertainties reflect the absolute accuracy of each individual determination. Relative uncertainties, especially for adjacent cluster sizes, should be substantially smaller, probably on the order of 0.1 eV or less, because systematic errors in the interpretations cancel.

The accuracy of these values can be qualitatively assessed by considering the observation that Co_nD^+ products decompose by losing D atoms, rather than Co atoms. This shows that $D_0(Co_n^+–D)$ should be less than $D_0(DCo_{n-1}^+–Co)$. This latter bond energy can be quantitatively equated with $D_0(Co_{n-1}^+–Co)+D_0(Co_n^+–D)–D_0(Co_{n-1}^+–D)$. Thus, if the bond energies, $D_0(Co_{n-1}^+–Co)$, are larger than $D_0(Co_{n-1}^+–D)$, then $D_0(Co_n^+–D)$ are less than $D_0(DCo_{n-1}^+–Co)$. It can be seen from Fig. 4 that $D_0(Co_{n-1}^+–Co)$ are indeed larger than our measured values of $D_0(Co_{n-1}^+–D)$ in all cases but $n=3$ where $D_0(Co_2^+–D) > D_0(Co_2^+–Co)$. Thus, except for $n=3$, the average $D_0(Co_n^+–D)$ values are qualitatively consistent with the decomposition patterns observed for these products.

In addition, we can consider our observation of dissociative chemisorption of D_2 on the clusters. These chemisorbed $Co_nD_2^+$ species are formed exothermically for clusters where n=4, 5, 10–16 indicating that $D_0(DCo_n^+–D)+D_0(Co_n^+–D) > 4.56\ eV = D_0(D_2)$. Assuming that the first and second cluster-deuterium bonds are roughly comparable, we should observe exothermic formation of $Co_nD_2^+$ when $D_0(Co_n^+–D) \geqslant D_0(D_2)/2 = 2.28$ eV, indicated by a line in Fig. 4. As can be seen from Table I and Fig. 4, the average $D_0(Co_n^+–D)$ values exceed this energy for $n \geqslant 9$. This is in qualitative agreement with our observation of $Co_nD_2^+$ products at thermal energies for the n=10–16 clusters. This criterion tends to suggest that the average values are more accurate than either loose PSL values (where those for $n \geqslant 12$ exceed 2.28 eV) or TTS values (where those for $n \geqslant 6$ exceed 2.28 eV). For smaller clusters, n=2, 4–8, $D_0(Co_n^+–D)$ values lie very close to 2.28 eV, within the uncertainty of the measurements, but are apparently not observed for n=2 and 6–8 because of their short lifetimes, as discussed above. For n=4 and 5, the observation of the $Co_4D_2^+$ and $Co_5D_2^+$ products at thermal energies suggests that these species have a second cluster-deuterium bond somewhat greater than the first.

B. Comparison of $D_0(Co_n^+–D)$ and $D_0(Co_n^+–Co)$

Figure 4 compares the cluster-deuteride bond energies derived in this study with metal–metal bond energies determined previously.[34] Overall, both $D_0(Co_n^+–D)$ and $D_0(Co_n^+–Co)$ generally increase as the cluster size increases, and they roughly parallel one another for many cluster sizes. However, the increase is nonmonotonic with local maxima at $Co_2^+–D$, $Co_4^+–D$, and $Co_6^+–D$ for cobalt–deuteride ionic clusters, and at $Co_5^+–Co$, $Co_7^+–Co$, $Co_{12}^+–Co$, and $Co_{14}^+–Co$ for pure metal clusters. As discussed above, $D_0(Co_n^+–Co)$ are stronger than $D_0(Co_n^+–D)$, except for n=2, as is seen easily from the difference of the bond energies, $D_0(Co_n^+–Co)–D_0(Co_n^+–D)$, also plotted as a function of cluster size in Fig. 4. It is known that first-row transition-metal deuteride cations have bonds that mainly involve 4s-1s interactions,[63] and it seems likely that this should also be true of larger clusters. Therefore, the differences between the $Co_n^+–D$ and $Co_n^+–Co$ bond energies suggest that $Co_n^+–Co$ bonding has strong contributions from both 4s-4s and 3d-3d interactions. This is similar to the trends observed for V_n^+ and Ni_n^+ clusters,[29,30] but distinct from the cases of Fe_n^+ and Cr_n^+ where $M_n^+–M$ and $M_n^+–D$ bond energies are more similar.[27,28] A quantitative comparison of these bond energies finds that cobalt–cobalt bonds are an average of 0.66±0.10 eV stronger than cobalt–deuterium bonds for n=1, 4, 6, 8–10, and 13. This increase can be attributed to metal–metal bonds enhanced by using 3d-3d interactions. For clusters, n=5, 7, 12, and 14, we speculate that there may be a geometric contribution to the $Co_n^+–Co$ bond energy variation. In analogy with our observations for iron,[27] chromium,[28] vanadium,[29] and nickel[30] clusters, this suggestion relies on the strong possibility that Co_6^+ (octahedron), Co_{13}^+ (icosahedral or octahedral with fcc or bcc packing), and Co_{15}^+ (bcc rhombic dodecahedron) clusters can have highly symmetric geometrical structures compared to neighboring clusters. Substitution of D for Co in these clusters breaks the symmetry, changing the molecular-orbital ordering, thereby leading to a less strongly bound system. For n=3, the $D_0(Co_3^+–Co)–D_0(Co_3^+–D)$ difference in bond ener-

gies is very small, 0.13 eV, which suggests that Co_4^+ clusters do not utilize $3d$-$3d$ bonding as efficiently as larger clusters.

In contrast with the larger clusters, the monomer and dimer of cobalt show trends in the Co_n^+–D and Co_n^+–Co bond energies that are inverted from one another. Because there is so little known about the geometric and electronic structures of cobalt cation clusters, we are left to speculate regarding a possible explanation. For the monomer, this is straightforward to understand. Ground-state $Co^+(^3F, 3d^8)$ can form a good $4s$-$4s$ covalent bond with ground-state $Co(^4F, 4s^2 3d^7)$ because the Co atom can donate two $4s$ electrons.[34,39] Thus, the ground state of Co_2^+, determined to be a $^6\Sigma$ state by electron-spin resonance (ESR) spectroscopy,[64] might have a $d\sigma_A^1 d\pi_A^4 d\delta_A^2 d\sigma_B^2 d\pi_B^4 d\delta_B^2 s\sigma_g^2$ configuration in the limit of atomiclike $3d$ orbitals or a $d\sigma_g^2 d\pi_u^4 d\delta_g^4 d\sigma_u^2 d\pi_g^2 d\sigma_u^1 s\sigma_g^2$ molecular configuration.[65] In contrast, a covalent $4s$-$1s$ bond in CoD^+ requires promotion of the Co^+ to a $4s^1 3d^7$ configuration, which takes 0.91 eV to promote and spin decouple the $4s$ electron from the $3d$ electrons.[41] Hence, $D_0(Co^+–D)$ is much weaker than $D_0(Co^+–Co)$. When binding D to Co_2^+, a singly occupied d orbital, such as the $d\sigma_u^1$, could make a strong covalent bond with a D $(1s^1)$ atom without any costly promotion. Alternatively, if bonding of D to a $4s$-like cluster orbital is needed, the relatively strong Co_2^+–D bond energy suggests that promotion of a d electron to a $4s$-like orbital is not very costly, which may be because little exchange energy is lost in forming such a covalent bond, unlike for CoD^+. As noted elsewhere,[34] larger cobalt clusters are generally considered to be formed by addition of cobalt atoms in $4s^1 3d^8$ electronic configurations, a state that lies 0.42 eV above the ground state.[66] Thus, the promotion energy weakens the Co_2^+–Co bond energy.

C. Comparisons to bulk-phase thermochemistry

Having measured bond energies for cobalt cluster hydride cations, it is interesting to compare our experimental thermochemical values determined here with those obtained for bulk-phase surfaces. The experimental values for the binding of hydrogen on Co(0001) are 2.60 eV (Refs. 2,67) and 2.65 eV on Co(1010).[68] Density-functional theory calculation values[69] for hydrogen binding energies on Co(0001) at on-top, bridge, fcc hollow, hcp hollow, and subsurface positions are 2.05, 2.61–2.64, 2.89, 2.87–2.88, and 2.36–2.41 eV, respectively. The values for the bridge and hollow sites are in reasonable agreement with the experimental values. The average experimental value, 2.63 eV, is plotted in Fig. 4. There it can be seen that the Co_n^+–D bond energies for larger clusters $(n \geqslant 13)$ are very close to that for bulk-phase cobalt. Similarly good agreement[70] has been found for bond energies of D and O atoms binding to clusters of Fe_n^+,[27,71] Cr_n^+,[28,72] V_n^+,[29,73] and Ni_n^+[30,74] versus bulk-phase values. This correspondence indicates that chemical binding is largely a local phenomenon as long as clusters have enough electronic "flexibility" to form strong covalent bonds.

D. D_2 activation by Co_n^+

For the cationic clusters n=2, 3, 6–8, no dideuteride products were observed, a result that can be attributed to the lifetime effects of these species, as explained above. For clusters n=4, 5, 11–13, and 15, $Co_nD_2^+$ cross sections decrease monotonically with increasing energy. This means that the reactions have no obvious barriers, behavior characteristic of exothermic ion-molecule reactions.

As noted above, the formation of $Co_9D_2^+$ exhibits threshold behavior, and $Co_{10}D_2^+$, $Co_{14}D_2^+$, and $Co_{16}D_2^+$ exhibit both exothermic and endothermic features in their cross sections. We analyzed the $Co_9D_2^+$ cross section using Eq. (5), as well as the endothermic features in the cross sections for n=10, 14, and 16 after subtracting a model of the exothermic reactivity in these systems (using a simple power law). RRKM lifetime effects are not considered in these analyses because kinetic shifts cannot occur in the formation of the $Co_nD_2^+$ products, the transient intermediates formed in the collision between reactants. If the internal energies of the reactant cluster ions are presumed to help activate the D_2 bond, we obtain thresholds for $Co_9D_2^+$, $Co_{10}D_2^+$, $Co_{14}D_2^+$, and $Co_{16}D_2^+$ of 0.79±0.07, 0.88±0.09, 0.97±0.11, and 1.03±0.10 eV, respectively. The values of 0.24±0.08, 0.16±0.07, 0.14±0.07, and 0.14±0.07 eV, respectively, are obtained without including the internal energies of the reactant cluster ions in the analysis. The justification for excluding the internal energy in the analysis of the reactions relies on several ideas. First, theoretical studies of the reaction of the Ni_{13} cluster with D_2 showed that the rates of reaction are insensitive to the temperature of the cluster over the range of 0–300 K.[75] Similarly, the experimental results showed that the sticking probabilities of H_2 on Ni(111) surfaces,[76] an activated dissociative chemisorption process, are independent of the surface temperature. Finally, excluding the internal energy yielded the most reasonable thermochemistry for the analogous products, $Fe_nD_2^+$, $Cr_nD_2^+$, and $V_nD_2^+$, in our previous cluster hydrogenation studies,[27–29] and does so in the present system as well, as seen from the following analysis.

If the thresholds for these clusters correspond to the endothermicity for dissociative chemisorption, then $D_0(DCo_n^+–D)$ bond energies can be derived using Eq. (7),

$$D_0(DCo_n^+–D) = D_0(D_2) - E_0(2) - D_0(Co_n^+–D) = E_0(1) - E_0(2). \quad (7)$$

If we use threshold analyses that do not consider the internal energy of the clusters to be available for reaction, $D_0(DCo_n^+–D)$ values obtained for n=9, 10, 14, and 16 are 1.97±0.34, 1.94±0.36, 1.77±0.36, and 1.74±0.38 eV, respectively, about 0.7±0.3 eV lower than the analogous $D_0(Co_n^+–D)$ bond energies. [If the internal energy is included in the threshold determinations, then the $D_0(DCo_n^+–D)$ values obtained are even lower, 1.42±0.34, 1.22±0.36, 0.94±0.37, and 0.84±0.39 eV, respectively.] For larger clusters, it is difficult to believe that a second D atom cannot find a binding site on the cluster comparable to the first D atom. Indeed, studies by Liu *et al.*[77] have found that iron cluster-D atom BDEs are comparable up to the limit where the clusters are saturated with D atoms. In analogy with arguments used previously for Fe_n^+,[27] Cr_n^+,[28] and V_n^+[29] clusters, we suggest that the thresholds measured here correspond to barrier heights

TABLE II. Thermal rate constants (10^{-10} cm^3/s) for reactions of cobalt clusters with D_2.

	Co_n^+		Co_n		
n	This work[a]	Ref. 12[b]	Ref. 9[c]	Ref. 7[d]	Ref. 11[e]
3	<0.005	0.53		0.89	
4	0.016	0.80		0.21	
5	0.094	1.5		0.080	
6	<0.005	0.53		0.021	
7	<0.005	0.40		0.029	
8	<0.005	0.27		0.063	
9	<0.005	0.53	0.05	0.096	
10	0.21	1.3	1.2	0.60	0.38
11	6.0	3.5	2.1	1.2	0.71
12	6.6	4.7	2.1	1.3	0.70
13	6.0	5.3	1.1	1.6	0.97
14	3.8	7.7	0.50	1.2	0.21
15	8.0	8.0	3.0	1.8	1.4
16	7.2	6.9	2.3	2.3	0.84
17		6.9	1.7	1.7	0.61
18		3.5	0.78	1.4	0.28
19		2.1	0.25	0.60	0.14
20		1.7	0.18	0.38	0.073
21		1.6	0.30	0.63	0.15
22		1.7		0.51	0.23

[a]Absolute rate constants for reaction of Co_n^+ with D_2 measured here under single-collision conditions. Uncertainties are ±30%.
[b]Relative reactivities for reaction of Co_n^+ with D_2, scaled to the value for Co_{15}^+ from the present work, see text. Estimated uncertainties are about ±30%.
[c]Absolute rate constants for reaction of Co_n with D_2. The accuracy of the rate constants is ±50%.
[d]Relative rates for reaction of Co_n with D_2, scaled to the value of Co_{16} from Ho *et al.* (Ref. 9) Estimated uncertainties are ±20%.
[e]Absolute rate constants for reaction of Co_n with D_2, calculated from the reported reaction probabilities, see text. Uncertainties are ±20%–30%.

along the potential energy surfaces for chemisorption, which means that the $D_0(DCo_n^+\text{-}D)$ bond energies for n=9, 10, 14, and 16 obtained above are only lower limits. Importantly, the conclusions that there are small activation barriers for the formation of $Co_9D_2^+$ and $Co_{14}D_2^+$ parallel the observations of Ho *et al.* for neutral clusters.[9] Of the neutral Co_n (n=9–21) clusters, only Co_9 and Co_{14} exhibited rate constants that increased at high and low temperatures, indicating a barrier to reaction. Temperature-dependent studies determined these barriers as 0.09 and 0.08 eV, respectively, somewhat smaller than those determined here for the cationic analogs, but of the same order of magnitude as the thresholds determined without including internal energies.

We now return to why dual-featured cross sections are observed for $Co_{10}D_2^+$, $Co_{14}D_2^+$, and $Co_{16}D_2^+$. As discussed above, the endothermic features are attributed to activation barriers for these processes, whereas the exothermic features probably correspond to populations of reactant trajectories that allow the internal energy of the clusters to couple with the reaction coordinate. Compared to the LGS cross section, the exothermic features in the cross sections for $Co_{10}D_2^+$, $Co_{14}D_2^+$, and $Co_{16}D_2^+$ are 2%, 35%, and 62% of the collision limit. Presumably the percentages increase with cluster size because the lifetime of a transient $Co_n(D_2)^+$ species should increase with cluster size, thereby allowing more efficient coupling of the internal energy into the reaction coordinate. This lifetime effect also explains why the $Co_nD_2^+$ cross sections for n=11–13 and 15 gradually increase with cluster size and why the energy at which the cross section declines rapidly (Fig. 2) moves to higher energy with cluster size.

E. Rate constants for $Co_nD_2^+$ formation

Cross sections can be converted to reaction-rate constants by using the expression,

$$k(\langle E\rangle) = \nu\sigma(E), \tag{8}$$

where $\nu=(2E/\mu)^{1/2}$ and $\mu=mM/(m+M)$, the reduced mass of the reactants. The rate constants depend on the mean energy of the reactants, which includes the average thermal motion of the neutral, such that $\langle E\rangle=E+(3/2)\gamma k_B T$, where $\gamma=M/(m+M)$. Table II and Fig. 5 show our absolute rate constants for reactions of cobalt cation clusters Co_n^+ with D_2 to form $Co_nD_2^+$ under single-collision conditions and thermal energies. In general, the rate constants for clusters n=4, 5, and 10 are small, over one order of magnitude lower than those for n=11–16, which are about two-thirds of the LGS value[44] of 9.55×10^{-10} cm^3 s^{-1}. On the basis of the noise level of these experiments, we can also put a lower limit of 5×10^{-13} cm^3 s^{-1} on the rate constants for reactions of n=2, 3, and 6–9.

Although the rates of neutral and cationic cobalt clusters reacting with D_2 need not be similar, it is of interest to make

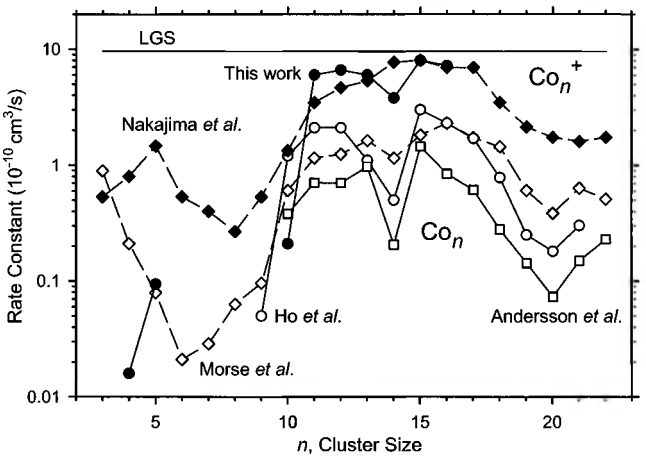

FIG. 5. Rate constants for cobalt cluster reactions with D_2 at thermal energy. The solid symbols indicate the results for cobalt cluster cations from the present study (circles, absolute values) and those of Ref. 12 (diamonds, relative values scaled to our value for Co_{15}^+). The experimental values for neutral cobalt clusters are indicated by the open circles (absolute rate constants from Ref. 9), the open diamonds (relative rate constants from Ref. 7, scaled to the value for Co_{16} from Ref. 9), and the open squares (values calculated from absolute reaction probabilities from Ref. 11, see text). The horizontal line indicates the LGS value for the collision rate constant (Ref. 44).

such a comparison. Figure 5 and Table II compare our rate constants with the experimental results from previous work on the reactions of cation[12] and neutral[7,9,11] cobalt clusters with D_2. Relative reactivities for cobalt cationic clusters from Nakajima *et al.*[12] are compared to our values by scaling these to the value of Co_{15}^+, the most reactive cluster in both studies. As seen from Fig. 5, the rate constants for $n=11$–16 are in good agreement with those measured here (although they do not observe a dip in the reactivity at $n=14$), whereas the values for $n=4$, 5, 10 are about one order of magnitude larger than our results. Note that the relative rate constants for Co_4^+, Co_5^+, and Co_{10}^+ are comparable in the two studies, but in contrast with the present observations, Nakajima *et al.*[12] found finite reactivity for cobalt cation clusters $n=3$, 6–9 at thermal energies. The difference in behavior for the small clusters ($n=3$–10) presumably lies in timescales for the two experiments and the higher-pressure conditions used by Nakajima *et al.*, which may allow collisional stabilization of physisorbed Co_n^+–D_2 adducts. For large clusters that already react with near unit efficiency, such effects would not alter the observed reactivities.

Absolute rate constants for neutral cobalt clusters were measured by Ho *et al.*[9] using a flow tube reactor (Fig. 5 and Table II). Persson *et al.*[11] have reported the absolute probabilities for reaction of neutral cobalt clusters with D_2 under near single-collision conditions. These are converted to absolute rate constants by using Eq. (8) with reaction cross sections approximated by multiplying the reported reaction probabilities by the Co_n–D_2 hard-sphere cross section, $\sigma_{HS}=\pi(1.38n^{1/3}+1.84)^2$.[11] As shown in Fig. 5, these show a very similar size dependence as the results of Ho *et al.* but are generally about a factor of two smaller (average ratio is 0.44 ± 0.16). In addition, the relative values from the study Morse *et al.*[7] are also shown in Fig. 5 by scaling these to the value of Co_{16} from the study Ho *et al.*[9] As seen from Fig. 5, all three sets of rate constants for the neutral cobalt clusters show similar patterns of reactivity and relative values are in reasonable agreement. In all of these studies, a dip in the reactivity at the Co_{14} cluster is found, paralleling that observed in our work. The comparison of cationic and neutral cobalt clusters shows that the patterns of the reactivities with cluster size are quite similar except for the smaller clusters, although the reactivities of the cationic clusters $n=11$–22 are about seven times larger than those of the corresponding neutral clusters. This enhancement can be attributed to the longer-range ion-induced dipole potential that increases the likelihood of collisions between cationic clusters and D_2 compared to the neutral analogs. The parallel reactivity patterns indicate that the intrinsic reactivity of the clusters is largely independent of the charge state. Not unexpectedly, the differences in the rate constants for smaller clusters indicate that changes in the electronic structure are more prominent and do affect the reactivity here.

F. Comparison of D_2 activation on other metal cluster cations

The reactions of Fe_n^+ ($n=2$–15), Cr_n^+ ($n=2$–14), V_n^+ ($n=2$–13), and Ni_n^+ ($n=2$–16) cluster cations with D_2 have been investigated previously.[27–30] In all the metal systems, dideuteride products, $M_nD_2^+$, are not formed in the reactions of smaller clusters because the lifetimes of the adducts are too short to observe experimentally. Once the clusters become sufficiently large, $n\geq9$ for Fe, $n\geq6$ for Cr, $n\geq4$ for V, $n\geq5$ for Ni, $n=4$, 5, and $n\geq9$ for Co, the $M_nD_2^+$ adducts are formed at low energies. For Fe_9^+, Cr_n^+($n=6$–8), V_n^+ ($n=4$, 5, 7, 9), Ni_n^+ ($n\geq5$), and Co_n^+ ($n=4$, 5, 11–13, 15) clusters, the cross sections of the dideuteride ions exhibit no barriers to reaction, whereas in all other cases, the cross sections exhibit only an endothermic feature or an endothermic feature combined with an exothermic tail. These latter processes are clearly activated ones requiring the input of energy to occur efficiently. Overall, there are many similarties in the reactions of V_n^+, Cr_n^+, Fe_n^+, Co_n^+, and Ni_n^+ with D_2, but patterns in reactivity (especially for small clusters) and thermochemistry are distinct for each metal system.

ACKNOWLEDGMENT

This work is supported by the Chemical Sciences, Geosciences, and Biosciences Division, Office of Basic Energy Sciences, Office of Science, U. S. Department of Energy.

[1] J. W. Davenport and P. J. Estrup, in *The Chemical Physics of Solid Surfaces and Heterogeneous Catalysis*, edited by D. A. King and D. P. Woodruff (Elsevier, New York, 1990), Vol. 3, p. 1.
[2] K. Christmann, Surf. Sci. Rep. **9**, 1 (1988).
[3] M. D. Morse, Chem. Rev. (Washington, D.C.) **86**, 1049 (1986); M. M. Kappes, *ibid.* **88**, 372 (1988).
[4] D. C. Parent and S. L. Anderson, Chem. Rev. (Washington, D.C.) **92**, 1541 (1992); M. P. Irion, Int. J. Mass Spectrom. Ion Processes **121**, 1 (1992); M. B. Knickelbein, Annu. Rev. Phys. Chem. **50**, 79 (1999).
[5] A. W. Castleman, Jr. and K. H. Bowen, Jr., J. Phys. Chem. **100**, 12911 (1996).
[6] P. B. Armentrout, J. B. Griffin, and J. Conceição, in *Progress in Physics of Clusters*, edited by G. N. Chuev, V. D. Lakhno, and A. P. Nefedov (World Scientific, Singapore, 1999), p. 198; P. B. Armentrout, Annu. Rev. Phys. Chem. **52**, 423 (2001).

[7]M. D. Morse, M. E. Geusic, J. R. Heath, and R. E. Smalley, J. Chem. Phys. **83**, 2293 (1985); M. E. Geusic, M. D. Morse, and R. E. Smalley, *ibid.* **82**, 590 (1984).
[8]J. Conceição, R. T. Laksonen, L.-S. Wang, T. Guo, P. Nordlander, and R. E. Smalley, Phys. Rev. B **51**, 4668 (1995).
[9]J. Ho, L. Zhu, E. K. Parks, and S. J. Riley, Z. Phys. D: At., Mol. Clusters **26**, 331 (1993); J. Chem. Phys. **99**, 140 (1993).
[10]E. K. Parks, G. C. Nieman, and S. J. Riley, Surf. Sci. **355**, 127 (1996).
[11]J. L. Persson, M. Andersson, and A. Rosén, Z. Phys. D: At., Mol. Clusters **26**, 334 (1993); M. Andersson, J. L. Persson, and A. Rosén, J. Phys. Chem. **100**, 12222 (1996).
[12]A. Nakajima, T. Kishi, Y. Sone, S. Nonose, and K. Kaya, Z. Phys. D: At., Mol. Clusters **19**, 385 (1991).
[13]D. M. Cox, K. C. Reichmann, D. J. Trevor, and A. J. Kaldor, J. Chem. Phys. **88**, 111 (1988).
[14]B. C. Guo, K. P. Kerns, and A. W. Castleman, Jr., J. Chem. Phys. **96**, 8177 (1992); J. Phys. Chem. **96**, 6931 (1992).
[15]D. B. Jacobson and B. S. Freiser, J. Am. Chem. Soc. **108**, 27 (1986); R. B. Freas, B. I. Dunlap, B. A. Waite, and J. E. Campana, J. Chem. Phys. **86**, 1276 (1986).
[16]E. Kapiloff and K. M. Ervin, J. Phys. Chem. A **101**, 8460 (1997).
[17]P. J. Brucat, C. L. Pettiette, L.-S. Zheng, M. J. Craycraft, and R. E. Smalley, J. Chem. Phys. **85**, 4747 (1986); E. K. Parks, L. Zhu, J. Ho, and S. J. Riley, Z. Phys. D: At., Mol. Clusters **26**, 41 (1993); J. Ho, E. K. Parks, L. Zhu, and S. J. Riley, J. Chem. Phys. **201**, 245 (1995).
[18]S. Nonose, Y. Sone, N. Kikuchi, K. Fuke, and K. Kaya, Chem. Phys. Lett. **158**, 152 (1989); M. P. Iron, P. Schnabel, and A. Selinger, Ber. Bunsenges. Phys. Chem. **94**, 1291 (1990).
[19]Y. H. Pan, K. Sohlberg, and D. P. Radge, J. Am. Chem. Soc. **113**, 2406 (1991); D. P. Ridge, in *Unimolecular and Bimolecular Ion-Molecule Reaction Dynamics*, edited by C. Y. Ng, T. Baer, and I. Powis (Wiley, Chichester, 1994), p. 337.
[20]A. M. L. Oiestad and E. Uggerud, Chem. Phys. **262**, 169 (2000).
[21]T. D. Klots, B. J. Winter, E. K. Parks, and S. J. Riley, J. Chem. Phys. **92**, 2110 (1990); **95**, 8919 (1991); E. K. Parks, B. J. Winter, T. D. Klots, and S. J. Riley, *ibid.* **96**, 8267 (1992); **99**, 5831 (1993).
[22]B. J. Winter, T. D. Klots, E. K. Parks, and S. J. Riley, Z. Phys. D: At., Mol. Clusters **19**, 375 (1991); **19**, 381 (1991); S. J. Riley, Ber. Bunsenges. Phys. Chem. **96**, 1104 (1992).
[23]M. A. Vannice, Catal. Rev. - Sci. Eng. **14**, 153 (1976); R. B. Anderson, *The Fischer-Tropsch Synthesis* (Academic, New Yorks, 1984).
[24]J. A. Moulijn, P. W. N. M. v. Leeuwen, and R. A. v. Santen, *Catalysis: An Integrated Approach to Homogeneous, Heterogeneous and Industrial Catalysis* (Elsevier, Amsterdam, 1993).
[25]J. Geerlings, M. C. Zonnevylle, and C. P. M. de Groot, Surf. Sci. **241**, 302 (1991); Surf. Sci. **241**, 315 (1991).
[26]E. Iglesia, Appl. Catal., A **161**, 59 (1997); H. Schulz, *ibid.* **186**, 3 (1999).
[27]J. Conceicao, S. K. Loh, L. Lian, and P. B. Armentrout, J. Chem. Phys. **104**, 3976 (1996).
[28]J. Conceicao, R. Liyanage, and P. B. Armentrout, Chem. Phys. **262**, 115 (2000).
[29]R. Liyanage, J. Conceicao, and P. B. Armentrout, J. Chem. Phys. **116**, 936 (2002).
[30]F. Liu, R. Liyanage, and P. B. Armentrout, J. Chem. Phys. **117**, 132 (2002).
[31]S. K. Loh, D. A. Hales, L. Lian, and P. B. Armentrout, J. Chem. Phys. **90**, 5466 (1989).
[32]T. G. Deitz, M. A. Duncan, D. E. Powers, and R. E. Smalley, J. Chem. Phys. **74**, 6511 (1981).
[33]S. K. Loh, D. A. Hales, and P. B. Armentrout, Chem. Phys. Lett. **129**, 527 (1986).
[34]D. A. Hales, C. X. Su, and P. B. Armentrout, J. Chem. Phys. **100**, 1049 (1994).
[35]E. Teloy and D. Gerlich, Chem. Phys. **4**, 417 (1974); D. Gerlich, Adv. Chem. Phys. **82**, 1 (1992); D. Gerlich, in *State-selected and State-to-state Ion-Molecule Reaction Dynamics*, edited by C.-Y. Ng and M. Baer (Wiley, New York, 1992), p. 1.
[36]K. M. Ervin and P. B. Armentrout, J. Chem. Phys. **83**, 166 (1985).
[37]N. R. Daly, Rev. Sci. Instrum. **31**, 264 (1959).
[38]N. Aristov and P. B. Armentrout, J. Am. Chem. Soc. **108**, 1806 (1986).
[39]D. A. Hales and P. B. Armentrout, J. Cluster Sci. **1**, 127 (1990).
[40]H. Huber and G. Herzberg, *Constants of Diatomic Molecules* (Van Nostrand Reinhold, New York, 1979).
[41]J. L. Elkind and P. B. Armentrout, J. Phys. Chem. **90**, 6576 (1986).
[42]P. Siegbahn, M. Blomberg, I. Panas, and U. Wahlgren, Theor. Chim. Acta **75**, 143 (1989).
[43]P. B. Armentrout, in *Selective Hydrocarbon Activation: Principles and Progress*, edited by J. A. Davies, P. L. Watson, J. F. Liebman, and A. Greenberg (VCH, New York, 1990), p. 467.
[44]G. Gioumousis and D. P. Stevenson, J. Chem. Phys. **29**, 294 (1958).
[45]W. J. Chesnavich and M. T. Bowers, J. Phys. Chem. **83**, 900 (1979).
[46]P. B. Armentrout, in *Advances in Gas Phase Metal Ion Chemistry*, edited by N. G. Adams and L. M. Babcock (JAI, Greenwich, 1992), Vol. 1, p. 83.
[47]P. B. Armentrout, Int. J. Mass. Spectrom. **200**, 219 (2000).
[48]L. Lian, C. X. Su, and P. B. Armentrout, J. Chem. Phys. **97**, 4072 (1992).
[49]R. G. Gilbert and S. C. Smith, *Theory of Unimolecular and Recombination Reactions* (Blackwell Scientific, Oxford, 1990).
[50]K. A. Holbrook, M. J. Pilling, and S. H. Robertson, *Unimolecular Reactions*, 2nd ed. (Wiley, New York, 1996).
[51]D. G. Truhlar, B. C. Garrett, and S. J. Klippenstein, J. Phys. Chem. **100**, 12771 (1996).
[52]M. T. Rodgers, K. M. Ervin, and P. B. Armentrout, J. Chem. Phys. **106**, 4499 (1997).
[53]F. Muntean and P. B. Armentrout, J. Chem. Phys. **115**, 1213 (2001).
[54]A. A. Shvartsburg, K. M. Ervin, and J. H. Frederick, J. Chem. Phys. **104**, 8458 (1996).
[55]R. J. Birgenean, J. Cordes, G. Dolling, and A. D. Woods, Phys. Rev. **136**, A1359 (1964).
[56]G. Simmons and H. Wang, *Single Crystal Elastic Constants and Calculated Aggregate Properties: A Handbook*, 2nd ed. (MIT, Cambridge, 1971).
[57]N. W. Ashcroft and N. D. Mermin, *Solid State Physics* (Saunders College, Philadelphia, 1976), p. 461.
[58]R. Röhlsberger, W. Sturhahn, T. S. Toellner, K. W. Quast, M. Hwssion, M. Hu, J. Sutter, and E. E. Alp, J. Appl. Phys. **86**, 584 (1999).
[59]R. L. Rubinovitz and E. R. Nixon, J. Phys. Chem. **90**, 1940 (1986).
[60]R. L. Rubinovitz, T. A. Cellucci, and E. R. Nixon, Spectrochim. Acta, Part A **43**, 647 (1987).
[61]M. E. Weber, J. L. Elkind, and P. B. Armentrout, J. Chem. Phys. **84**, 1521 (1986).
[62]P. B. Armentrout, in *Structure/Reactivity and Thermochemistry of Ions*, edited by P. Ausloos and S. G. Lias (D. Reidel, Dordrecht, 1987), p. 97.
[63]P. B. Armentrout and B. L. Kickel, in *Organometallic Ion Chemistry*, edited by B. S. Freiser (Kluwer Academic, Dordrecht, 1996), p. 1.
[64]R. J. Van Zee, Y. M. Hamrick, S. Li, and W. Weltner, Jr., Chem. Phys. Lett. **195**, 214 (1992).
[65]L. M. Russon, S. A. Heidecke, M. K. Brike, J. J. Conceicao, P. B. Armentrout, and M. D. Morse, Chem. Phys. Lett. **204**, 235 (1993); L. M. Russon, S. A. Heidecke, M. K. Brike, J. J. Conceicao, M. D. Morse, and P. B. Armentrout, J. Chem. Phys. **100**, 4747 (1994).
[66]J. Sugar and C. Corliss, J. Phys. Chem. Ref. Data Suppl. **14**, 1 (1985).
[67]M. E. Bridge, C. M. Comrie, and R. M. Lambert, J. Catal. **58**, 28 (1979).
[68]K. H. Ernst, E. Schwarz, and K. Christmann, J. Chem. Phys. **101**, 5388 (1994).
[69]D. J. Klinke and L. J. Broadbelt, Surf. Sci. **429**, 169 (1999).
[70]P. B. Armentrout, Eur. J. Mass Spectrom. **9**, 531 (2003).
[71]J. B. Griffin and P. B. Armentrout, J. Chem. Phys. **106**, 4448 (1997).
[72]J. B. Griffin and P. B. Armentrout, J. Chem. Phys. **108**, 8062 (1998).
[73]J. Xu, M. T. Rodgers, J. B. Griffin, and P. B. Armentrout, J. Chem. Phys. **108**, 9339 (1998).
[74]D. Vardhan, R. Liyanage, and P. B. Armentrout, J. Chem. Phys. **119**, 4166 (2003).
[75]J. Jellinek and Z. B. Guvenc, Z. Phys. D: At., Mol. Clusters **26**, 110 (1993); in *Physics and Chemistry of Finite Systems: From Clusters to Crystals*, edited by P. Jena, S. N. Khanna, and B. K. Rao (Kluwer, Boston, 1992), Vols. I and II, p. 1047;in *Mode Selective Chemistry*, edited by J. Jortner, R. D. Levine, and B. Ullman (Kluwer, Boston, 1991), p. 153.
[76]H. J. Robota, W. Vielhaber, M. C. Lin, J. Segner, and G. Ertl, Surf. Sci. **155**, 101 (1985).
[77]K. Liu, E. K. Parks, S. C. Richtsmeier, L. G. Pobo, and S. J. Riley, J. Chem. Phys. **83**, 2882 (1985).